An Ankle-Foot Prosthesis Emulator with Control of Plantarflexion and Inversion-Eversion Torque

Myunghee Kim, Tianjian Chen, Tianyao Chen and Steven H. Collins*

***Abstract*—Ankle inversion-eversion compliance is an important feature of conventional prosthetic feet, and control of inversion, or roll, in active prostheses could improve balance for people with amputation. We designed a tethered ankle-foot prosthesis with two independently-actuated toes that are coordinated to provide plantarflexion and inversion-eversion torques. A Bowden cable tether provides series elasticity. The prosthesis is simple and lightweight, with a mass of 0.72 kg. Strain gauges on the toes measure torque with less than 1% RMS error. Benchtop tests demonstrated a rise time of less than 33 ms, peak torques of 250 N·m in plantarflexion and ±30 N·m in inversion-eversion, and peak power above 3 kW. The phase-limited closed-loop torque bandwidth is 20 Hz with a chirp from 10 to 90 N·m in plantarflexion, and 24 Hz with a chirp from −20 to 20 N·m in inversion. The system has low sensitivity to toe position disturbances at frequencies of up to 18 Hz. Walking trials with an amputee subject demonstrated RMS torque tracking errors of less than 5.1 N·m in plantarflexion and less than 1.5 N·m in inversion-eversion. These properties make the platform suitable for testing inversion-related prosthesis features and controllers in experiments with humans.**

***Index Terms*—Medical Robots and Systems, Rehabilitation Robotics, Mechanism Design, Prosthetics, Locomotion**

I. Introduction

Robotic prostheses can improve locomotor performance for individuals who have restricted mobility due to lower-limb amputation. During walking, these devices can restore normal ankle and knee kinematics in the sagittal plane [1], reduce metabolic rate [2, 3], and provide direct neural control of the limb [4]. As robotic technologies improve, active prostheses are expected to enhance performance even further [5–7].

Ankle inversion-eversion control may be important to improving prosthesis function. Ankle inversion, or roll, moment has a strong effect on side-to-side motions of the body during walking. Side-to-side motions seem to require active balance [8–10], particularly for amputees [11]. During non-amputee walking, ankle muscles apply inversion moments to tune mediolateral center of pressure location and maintain balance [12, 13], including during the recovery from external disturbances [14]. However, ankle inversion moment patterns are altered in the prosthetic limb among individuals with amputation [15]. Many commercial prostheses feature a passive inversion-eversion degree of freedom, either using an explicit joint [16] or a flexure [17]. These passive joints can mitigate undesirable inversion moments created by uneven ground, but cannot provide the more sophisticated control thought to be used by humans. Difficulty controlling inversion-eversion torque in the prosthetic ankle may partially explain reduced stability [18] and increased fear of falling and fall rates [19] among people with amputation.

Robotic prosthesis designs have begun to incorporate active control of ankle inversion-eversion. Panzenbeck and Klute [20] describe a tethered ankle prosthesis with inversion provided by a four-bar linkage and controlled by a linear actuator. The device has a mass of 2.9 kg, can produce torques of up to 34 N·m, and has a 90% rise time of 0.180 s. A plantarflexion degree of freedom is provided using a passive spring. Ficanha et al. [21] describe a prototype device intended to provide both plantarflexion and inversion-eversion control using two motors and a gimbal joint. The device has a mass of 1.13 kg. Bellman et al. [22] describe a computer model of a similar device, with estimated mass of 2.1 kg. Devices with similar peak torque but lower mass and active control of both plantarflexion and inversion-eversion would enable experimental evaluation of a larger range of assistance techniques.

The mass and complexity of prostheses with inversion-eversion control is related to joint design and actuation approach. The human foot has dozens of physiological features that might help people to maintain balance during walking, including multi-axis joints, articulations that couple lean to yaw [23] and self-stiffening mechanisms [24]. However, mimicking such foot architecture would involve complicated mechanical elements such as linkages and gimbal joints. This often leads to large components with complex loading, resulting in increased strengthen and mass requirements. Independent, bidirectional actuation of both plantarflexion-dorsiflexion and inversion-eversion seems to require these bulky joint architectures. Actuators for these degrees of freedom are typically heavy, suggesting a relocated drive approach to reduce distal mass. However, bidirectional actuation makes drive relocation challenging. For example, bidirectional Bowden cable transmissions must be preloaded to prevent backlash, increasing losses from friction and nonlinearities from stiction. These

M. Kim is with the Department of Mechanical Engineering at Carnegie Mellon University, Pittsburgh, PA, 15213 USA and the John A. Paulson School of Engineering and Applied Sciences and Wyss Institute for Biologically Inspired Engineering at Harvard University, Cambridge, MA, 02138 USA. (e-mail: skyforme@gmail.com).

T. Chen is with the Department of Mechanical Engineering at Columbia University, New York, NY, 10025 USA (e-mail: tc2764@columbia.edu).

T. Chen is with the Department of Biomedical Engineering at The Catholic University of America, DC, 20064, (email: chentianyao@gmail.com).

S. H. Collins is with the Department of Mechanical Engineering and the Robotics Institute at Carnegie Mellon University, Pittsburgh, PA, 15213 USA and the Department of Mechanical Engineering, Stanford University, Stanford, CA 94305 USA.

This material is based on work supported by the National Science Foundation, Grant No. CMMI-1300804, all performed at Carnegie Mellon University.

*Corresponding author: S. H. Collins (e-mail: stevecollins@stanford.edu).

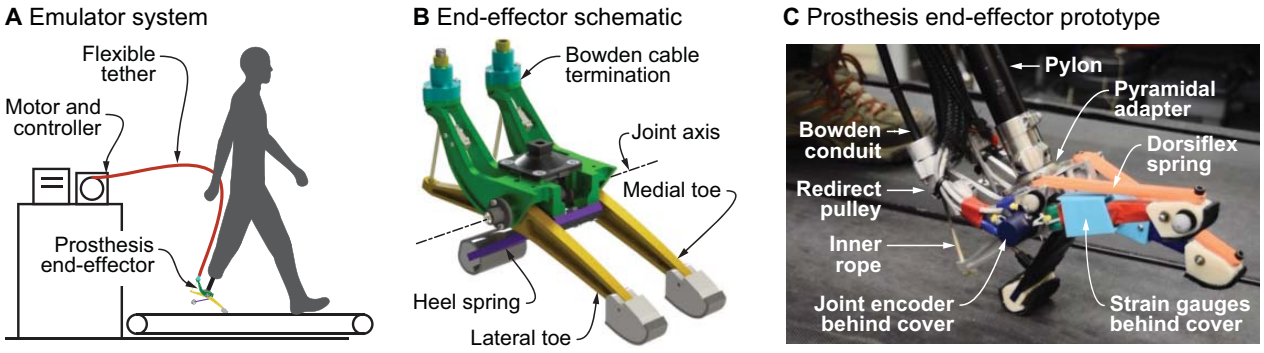

Fig. 1. Mechanical design of the two degree of freedom ankle-foot prosthesis emulator. **A** The emulator system consists of (1) powerful off-board actuation and control hardware, (2) a flexible Bowden cable tether, and (3) an end-effector worn by the user. **B** The prosthesis end-effector has two independently-actuated toes (yellow) that rotate about an axis in the frame (green) approximating the human ankle joint. A separate, passive heel spring (purple) rigidly connects to the frame. **C** The prototype used in experiments is instrumented with encoders at each ankle joint and four strain gauges in a Wheatstone bridge on each toe to measure torque. The device is connected to the user via a universal pyramidal adapter. Rubber bands dorsiflex toes during the swing phase of walking.

problems are difficult to overcome even in well-designed systems.

An alternative is suggested by the split-toe flexures in conventional passive prostheses and the actuation schemes in some powered ankle orthoses [25]. During walking, peak inversion-eversion torques are of much lower magnitude than peak plantarflexion torques [26], and the majority of the inversion impulse occurs during periods of high plantarflexion torque [27]. This may be in part due to the shape of the human foot, which has a wider toe than heel. Coupling plantarflexion and inversion-eversion torque through the actions of two hinged toes might therefore provide sufficient inversion capacity while allowing a simple, lightweight design. Such an approach would also lend itself to drive relocation, requiring only two unidirectional Bowden cables, half as many as in a fully-actuated case, and no preload.

Mechatronic performance in experimental prosthesis systems can also be improved by separating actuation hardware from worn elements. A tethered emulator approach [28–31] decouples the problems of discovering desirable prosthesis functionality from the challenges of developing fully autonomous systems. Powerful off-board motors and controllers are connected to lightweight instrumented end-effectors via flexible tethers, resulting in low worn mass, high torque, high power, and high-fidelity torque control [28, 29, 32, 33]. Such systems can be used to haptically render virtual prostheses to human users, facilitating the discovery of novel device behaviors [34, 35] that can then be embedded in separate autonomous designs [36]. This approach can also be used for rapid comparison of commercial prostheses in a clinical setting [31, 37]. To be most effective, such prosthesis emulators should have high closed-loop torque bandwidth and lightweight, strong, accurately-instrumented end-effectors.

Series elasticity can have a strong effect on the quality of torque control in a robotic emulator system. Adding a spring in series with a high-stiffness transmission can reduce sensitivity to unexpected actuator displacements [38] such as those imposed by the human. Unfortunately, series compliance also reduces force bandwidth when the output is fixed, because the motor must displace further to stretch the spring. The optimal stiffness strikes a balance between these competing factors for a particular system and task. In a tethered emulator, the flexible transmission itself may have significant compliance, which might provide appropriate series elasticity.

Here we describe the design and evaluation of a robotic ankle-foot prosthesis emulator system with active control of both plantarflexion and inversion-eversion torques. We designed an end-effector that allowed inversion-eversion using two articulated toes, which we aimed to make lightweight and strong. We integrated the end-effector with existing off-board motor and control hardware, expected to facilitate high-bandwidth torque control. The end-effector did not include explicit series elasticity, testing the sufficiency of axial compliance in the tether. We programmed a basic walking controller intended to evaluate the system's potential for emulating prosthesis behavior during interactions with a human user, such as devices with a range of stiffnesses in plantarflexion [28, 34] and inversion/eversion [39]. We expect this approach to result in validation of a system that can explore new dimensions of prosthesis assistance, particularly those related to balance during walking.

An earlier version of this work was presented at the *International Conference on Robotics and Automation* [40]. In this paper, we present the results of additional benchtop tests of peak torque and peak power, the results of additional walking trials with a subject with transtibial amputation, expanded methods, results, figures, tables and discussion, supplementary videos, and complete hardware designs, in the form of CAD models and catalog part numbers, as supplementary materials.

II. Methods

We designed and constructed an ankle-foot prosthesis end-effector with torque control in both plantarflexion and inversion-eversion directions. We characterized system performance in benchtop tests, including peak torque, peak power, torque control bandwidth and disturbance rejection, and characterized torque tracking performance during walking under a variety of conditions with an amputee participant.

A. Mechanical Design

The two degree of freedom ankle-foot prosthesis was designed as an end-effector for a tethered emulator system

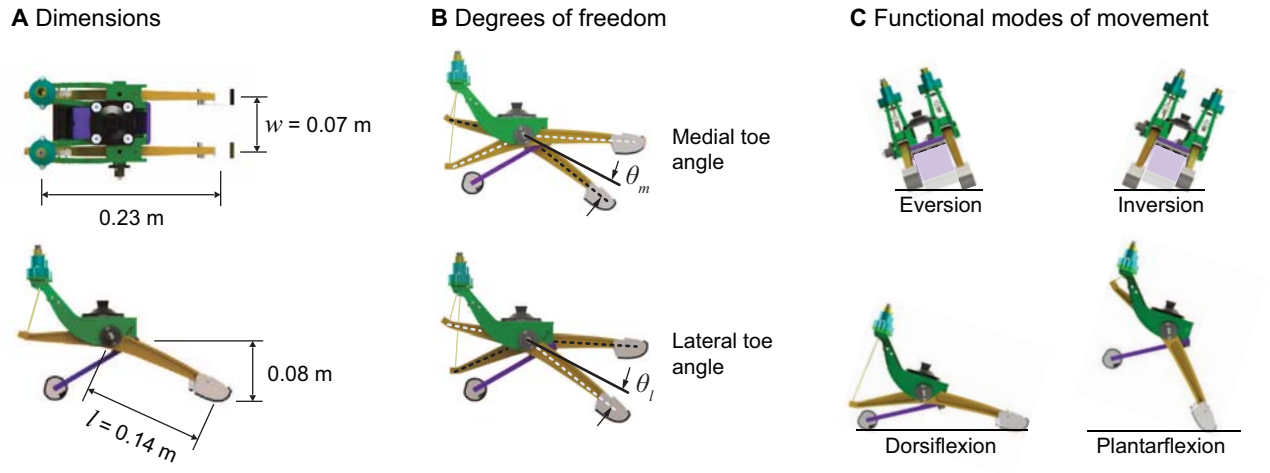

Fig. 2. Dimensions, degrees of freedom and functional modes of movement of the ankle-foot prosthesis end effector. **A** The prosthesis has dimensions similar to those of a human foot. The dimensions critical to torque control are foot width, w, and toe length, l. **B** The medial toe (yellow, black dashed highlight) and lateral toe (yellow, white dashed highlight) rotate about a joint in the frame (green), relative to a neutral position in which the toes touch the ground and the pylon is vertical (black line). This forms two independently actuated degrees of freedom. Toe torque is defined in the same direction as toe angle. The heel spring (purple) is rigidly connected to the frame, providing an additional passive degree of freedom. **C** Plantarflexion occurs when both toes rotate together and inversion-eversion occurs when the medial and lateral toes move in opposite directions. Plantarflexion and inversion-eversion torques are proportional to the sum and difference, respectively, of individual toe torques.

(Fig. 1A). Powerful actuation and control hardware is located off-board so as to keep worn mass low. Flexible Bowden cable tethers transmit mechanical power to the prosthesis, but do not interfere with natural movements of the limb.

The prosthesis end-effector consists of a frame, two toes with revolute joints, and a compliant heel. The toes share a single axis of rotation similar to the plantarflexion axis in the human ankle joint, and are spaced mediolaterally such that one is closer to the centerline of the body (Fig. 1B). The frame of the device is connected to the user's pylon or socket via a universal pyramidal adapter (Fig. 1C; Video 1).

The prosthesis frame houses needle roller bearings for the ankle joints, which have a double-shear construction. Each toe is long and thin, tapers towards its ends, and has an I-beam cross section, making it well-suited to three-point bending. One end of the toe contacts the ground, while the other end is acted on by the Bowden cable, with the hinge located in the middle. When the inner rope of the Bowden cable pulls upwards on the posterior aspect of the toe, a moment is generated. The Bowden cable conduit presses down on the frame equally and oppositely, such that the foot experiences no net force from the transmission itself. Rubber bands act to dorsiflex the toe when transmission forces are low, such as when the foot does not contact the ground. Several rubber band orientations were tested, all of which were found to be effective. A separate, unactuated heel spring is connected to the frame. Rubber-coated plastic pads are attached to the ends of the heel and toes to improve traction against the ground.

Prosthesis dimensions were based on an average male human foot [41]. The device measures 0.23 m in length, heel to toe, 0.07 m in width, toe center to toe center, and 0.08 m in height, from ground to ankle joint, in the neutral configuration (Fig. 2A). Toe length, from axis of rotation to tip, is 0.14 m. Ankle range of motion is -20° to 30° in plantarflexion and greater than -30° to 30° in inversion-eversion, relative to the neutral position in which the foot is flat on the floor and the pylon is vertical. This range of motion is greater than that observed during normal walking [42] and comparable to the range of the human ankle joint [43]. The prosthesis end-effector weighs 0.72 kg.

The prosthesis achieves torque and motion in both plantarflexion and inversion-eversion directions using two independent toes. Each toe rotates separately about the frame (Fig. 2B). Plantarflexion occurs when both toes rotate in the same direction, and inversion-eversion occurs when they rotate in opposite directions (Fig. 2C; Video 1). We define plantarflexion angle as the average of the toe angles and inversion-eversion angle as the difference between toe angles multiplied by the ratio of toe length to half the foot width. Similarly, plantarflexion torque, τ_{pf}, is defined as the sum of the lateral and medial toe torques, τ_l and τ_m, while inversion torque, τ_{inv}, is defined as the difference between the lateral and medial toe torques multiplied by the ratio of half the foot width, $\frac{1}{2}w$, to toe length, l, or

$$\begin{aligned} \tau_{pf} &= \tau_l + \tau_m \\ \tau_{inv} &= \tfrac{w}{2l}(\tau_l - \tau_m) \end{aligned} \tag{1}$$

We chose these definitions of plantarflexion and inversion-eversion torque because they are consistent with biomechanics nomenclature. These definitions also allow relatively simple instrumentation, requiring only single-axis torque sensing on each toe. Alternate torque definitions would require additional sensing capabilities. Defining torques in the ground reference frame, for example, would also require the measurement of axial and mediolateral toe forces, as well as the absolute orientation of the prosthesis.

This torque definition makes the approximation that the contact point of the toe is centered on the toe pad. Small differences in effective contact point can occur during walking, for example if the ankle is substantially everted and the toe

rolls onto one edge (Fig. 2C). However, toe width is small compared to foot width and the toe pad material is soft, both of which limit the mediolateral displacement of the center of pressure of the toe contact. Inaccuracies in measuring inversion-eversion moment in the prosthesis reference frame are therefore expected to be small.

Toes are actuated through independent Bowden cable tethers and off-board motors, allowing independent control of medial and lateral toes. Plantarflexion and inversion-eversion torques can be independently controlled, but maximum allowable inversion-eversion torque is proportional to plantarflexion torque. When inversion torque is zero, the plantarflexion torque is divided evenly between the toes. As inversion torque increases towards its limit, the torque on the lateral toe approaches the total desired plantarflexion torque, while the torque on the medial toe approaches zero. When inversion (or eversion) torque equals plantarflexion torque divided by the ratio of toe length to half the foot width, $\frac{2l}{w}$, the inversion-eversion torque cannot be increased further, since doing so would require negative torque on the medial (or lateral) toe, and negative ground reaction forces. This defines a feasible region of inversion torques as a function of plantarflexion torque: $|\tau_{inv}| \leq \frac{w}{2l}\tau_{pf}$. For torque patterns typical of human walking, inversion-eversion torques lie within the feasible region during most of stance (Fig. 3).

The end-effector did not include an explicit spring in the transmission, but some series elasticity was provided by the Bowden cable. Series elasticity can improve torque tracking in the presence of disturbances from the human user [44]. In our prior designs [28, 32], we used fiberglass leaf springs or steel coil springs at the connection between the Bowden cable and the hinged foot element, resulting in combined rotational stiffnesses of between 140 and 320 N·m·rad^{-1}. In this design, we explored whether the compliance of the Bowden cable itself might be sufficient to facilitate low-error torque tracking. This would have the benefit of reducing the mass and complexity of the end-effector. In tests where the off-board motors were fixed while the prosthesis toes were rotated, we measured an effective stiffness of about 550 N·m·rad^{-1}. With increased series stiffness, we expected joint torque to change more quickly when toes were fixed and the motor was rotated, resulting in higher closed-loop torque bandwidth. However, we also expected torques to change more quickly when the motor was stationary and the toes were unexpectedly rotated, for example during initial contact with the ground, which could result in poorer torque tracking under realistic conditions. We therefore separately tested bandwidth, disturbance rejection and torque tracking during walking, as described in the experimental methods below.

The prosthesis frame and toes were machined from 7075-T6 aluminum, the heel spring was machined from fiberglass (GC-67-UB, Gordon Composites, Montrose, CO, USA), and the toe pads were fabricated using fused-deposition modeling of ABS plastic. Off-board actuation was provided by two 1.61 kW AC servomotors with 5:1 planetary gearheads and dedicated motor drives (Baldor Electric Corp., Fort Smith, AR), controlled by a 1 GHz real-time controller (dSPACE Inc., Wixom, MI). Bowden cables had coiled-steel outer conduits (Lexco Cable Mfg., Norridge, IL) and 3 mm synthetic inner ropes (Vectran Fiber Inc., Fort Mill, SC). The motor, real-time controller and tether are described in detail in [29].

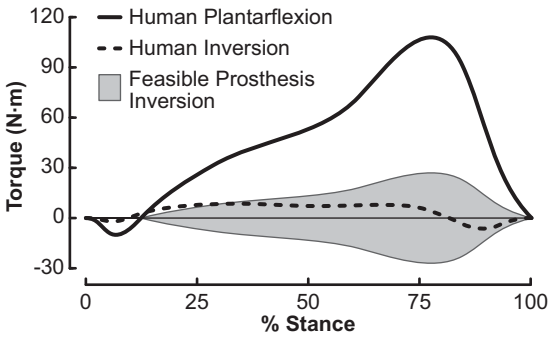

Fig. 3. Coupling between prosthesis plantarflexion and inversion-eversion torque illustrated with typical human walking data. Maximum feasible inversion-eversion torque (gray region) is proportional to plantarflexion torque (Eq. 1). With a typical plantarflexion torque pattern (solid line) the typical inversion-eversion torque (dashed line) falls within the feasible region for this device. Reference data for human walking at 1.6 m·s^{-1} are from [27].

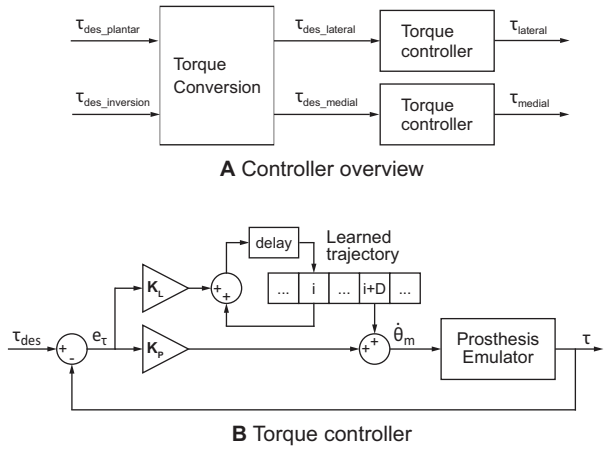

Fig. 4. **A** Desired plantarflexion and inversion/eversion torque were converted to the desired medial and lateral torque for each toe. Control actions are independently performed for each toe. **B** Block diagram illustrating the torque control approach for each toe. Desired torque, τ_{des}, is compared to measured torque, τ, to obtain torque error, e_τ. In the feedback loop, a proportional gain, $\mathrm{K_P}$, is applied to the error and used to set desired motor velocity, $\dot{\theta}_m$. The feed-forward compensation used during walking trials is updated by applying a learning gain, $\mathrm{K_L}$, to the torque error and adding the result to the existing value of the learned trajectory of motor velocity commands for this instant in time, i. The update takes effect on the next walking step. The previously-learned compensation is used to command desired motor velocity on this walking step, adding to the feedback loop. The feed-forward compensation value is from an instant D control-loop cycles in the future, reflecting an anticipated delay in achieving the desired motor velocity after it is commanded.

Medial and lateral toe joint angles were sensed individually using digital absolute magnetic encoders (MAE3, US Digital, Vancouver, WA). Toe torques were sensed using strain gauges (SGD-3, Omega Engineering, Stamford, CT), configured in a Wheatstone bridge, with two gauges on the top and bottom surfaces of each toe midway between the tip and the ankle joint. Heel contact was sensed using strain gauges on the heel spring (KFH-6, Omega Engineering), with a half bridge configuration. Bridge voltage was amplified (FSH01449, Futek, Irvine, CA), sampled at a frequency of 5000 Hz and low-

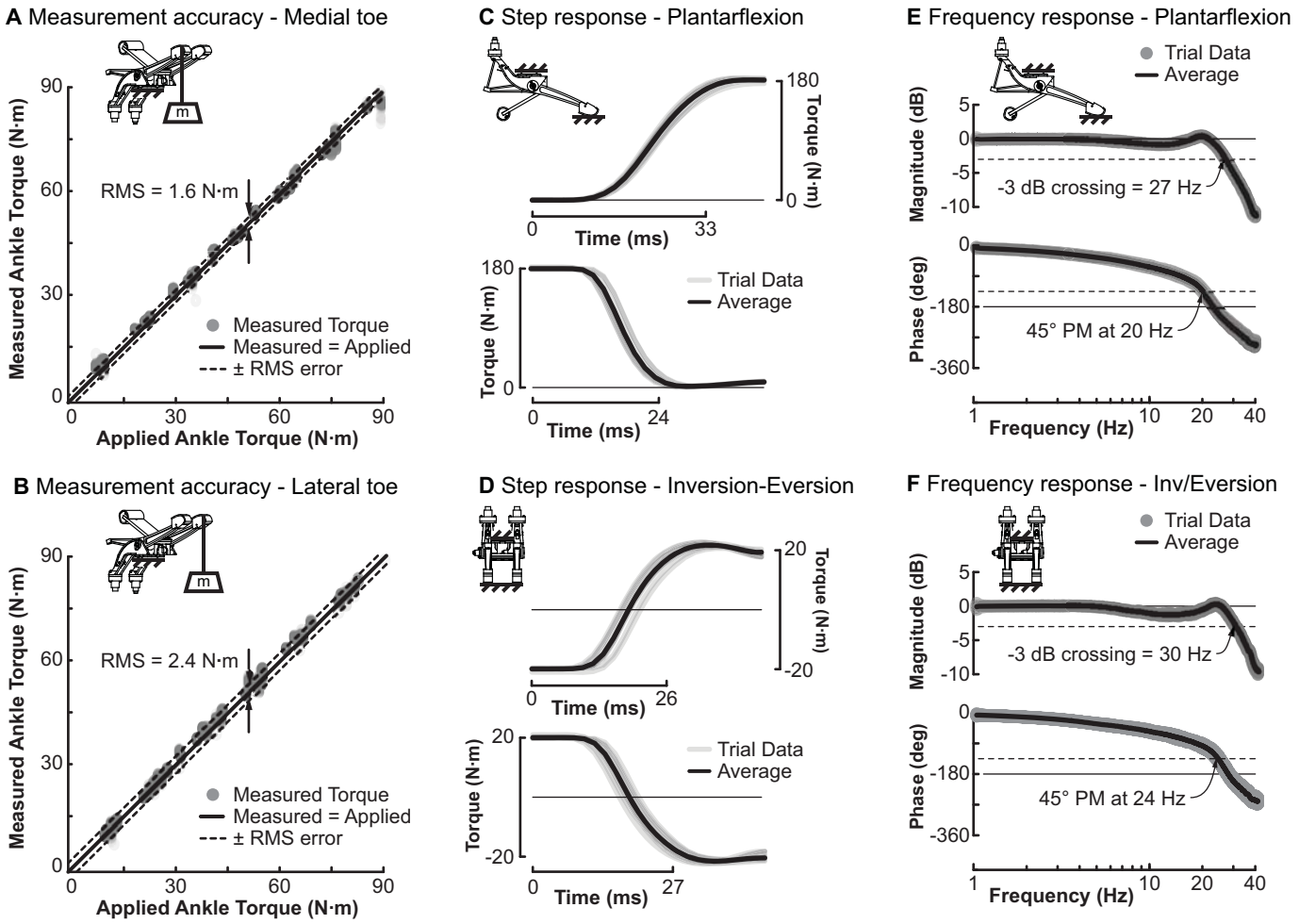

Fig. 5. Benchtop tests with a fixed load demonstrate low torque measurement error, fast rise time and high closed-loop torque bandwidth in both plantarflexion and inversion-eversion directions. Torque measurement validation for the **A** medial and **B** lateral toes. Step responses for closed-loop control of **C** plantarflexion and **D** inversion-eversion torque. Rise and fall times ranged from 0.024 to 0.033 s. Bode plots for closed-loop control of **E** plantarflexion and **F** inversion-eversion torque, calculated from responses to 90 N·m and $\pm$20 N·m magnitude chirps in desired torque, respectively. Bandwidth ranged from 20 to 30 Hz, limited by the 45° phase margin criterion.

pass filtered with a cutoff frequency of 100 Hz. Plantarflexion and inversion-eversion angles and torques were calculated in software from medial and lateral toe values.

A compressed archive with CAD models of each custom prosthesis component and a PDF bill of materials for all catalog components can be found at [45]. Off-board actuation designs, tether specifications, and example control software can be found as supplementary materials for [29] at [46].

B. Control

We used classical feedback control to regulate torque during benchtop tests, with an additional iterative learning term during walking trials (Fig. 4). Desired torque for each toe was first calculated from desired plantarflexion and inversion-eversion torques by solving Eq. (1).

$$\begin{aligned} \tau_l &= \tfrac{1}{2}(\tau_{pf} + \tfrac{w}{2l}\tau_{inv}) \\ \tau_m &= \tfrac{1}{2}(\tau_{pf} - \tfrac{w}{2l}\tau_{inv}) \end{aligned} \tag{2}$$

Motor velocities were then commanded using proportional control on toe torque error, $\dot{\theta}_m = K_p \cdot \tau_{des}$ in Fig. 4**B**. Motor velocity is similar to the rate of change in toe torque, owing to compliance in the Bowden cable transmission between the off-board motor and prosthesis toe. The transmission also introduced nonlinearities such as stiction, however, which we addressed using a model-free iterative learning controller. During walking trials, this time-based iterative learning term was added to the proportional control term, providing feed-forward compensation of torque errors that tended to occur at the same time each step. The iteratively learned compensation was updated on each step based on measured torque tracking errors. See the caption of Fig. 4 for more on this method, which is described in detail in [33].

In walking trials, torque control was used during stance and position control was used during swing. Initial toe contact was sensed from an increase in toe torque upon making contact with the ground. During the ensuing stance period, desired inversion-eversion torque was set to a constant value, providing a simple demonstration of platform capabilities. Desired plantarflexion torque during stance was calculated as a function of plantarflexion angle, as described in [47], so as to approximate the torque-angle relationship observed at the

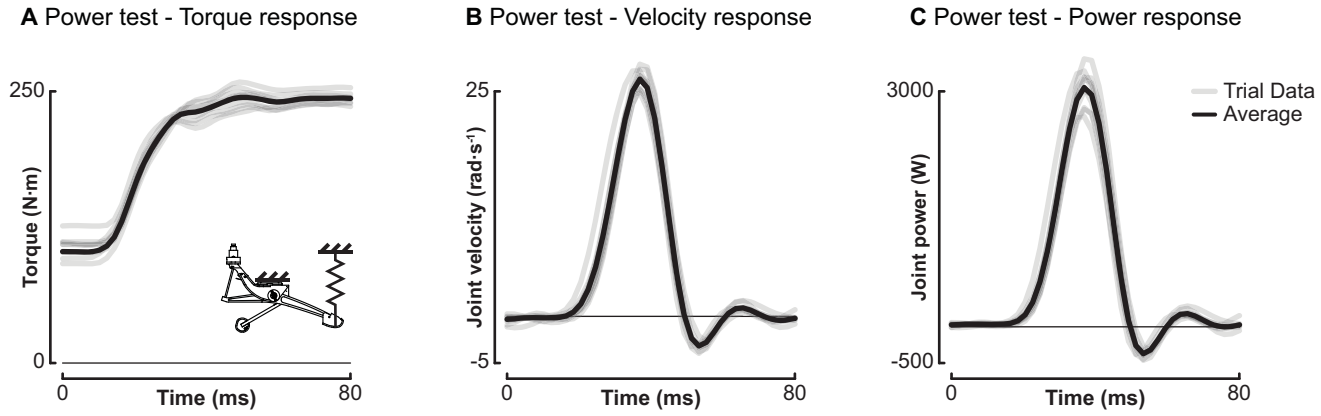

Fig. 6. Benchtop tests with a compliant load demonstrate high peak torque, velocity and power at the ankle joint. **A** Measured plantarflexion torque peaked at about 250 N·m. **B** Measured plantarflexion velocity peaked at above 25 rad·s^{-1}. **B** Measured joint mechanical power peaked at about 3 kW.

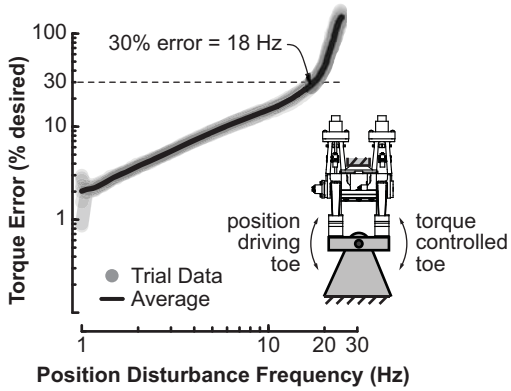

Fig. 7. Disturbance rejection, depicted as the relationship between torque error (% of the constant desired value) versus the frequency of an applied disturbance in toe position. This characterizes the ability of the system to reject unexpected environmental disturbances, such as from sudden contact with the ground. Torque error was less than 30% of the desired value of 30 N·m for disturbance frequencies up to 18 Hz.

ankle during normal walking [42]. Toe off was detected when plantarflexion torque crossed a minimum threshold. During the ensuing swing phase, toes were position controlled to provide ground clearance.

C. Experimental Methods

We conducted benchtop tests to characterize device performance in terms of torque measurement accuracy, response time, bandwidth, peak torque, peak power and disturbance rejection. We performed walking trials to assess mechatronic performance under similar conditions as expected during biomechanics experiments with amputee subjects.

C.1 Benchtop Testing Methods:

Torque measurement calibration was performed by applying known forces to the end of each toe using free weights and fitting amplified strain gauge bridge voltage to applied torque. Measurement accuracy was characterized in a separate validation test as root mean squared (RMS) error between applied and measured toe torques.

Step response tests were performed in which we rigidly fixed the prosthesis frame and toes and commanded desired torque as a square wave from 0 to 180 N·m in plantarflexion or -20 to 20 N·m in inversion-eversion. We conducted 10 trials for each direction and computed the mean and standard deviation of the 90% rise and fall times.

We performed bandwidth tests in which desired torque was commanded as a 0 to 40 Hz chirp, oscillating between 10 and 90 N·m for plantarflexion and between -20 and 20 N·m for inversion-eversion. We used an exponential chirp to improve signal to noise ratio in the low frequency range. We transformed the desired and measured torque into the frequency domain using a Fast Fourier Transform and used the magnitude ratio and phase difference to generate a Bode plot. We calculated the gain-limited and phase-limited bandwidths [48] as the frequencies at which the amplitude ratio was -3 dB and the phase margin was 45°, respectively. We performed 10 trials for both torques and calculated crossover frequency means and standard deviations.

Peak torque and peak power were characterized using step responses with a compliant load. We rigidly fixed the prosthesis frame to the benchtop and attached the toes to the benchtop through a coil spring with stiffness of 63,000 N·m^{-1}. We then commanded desired plantarflexion torque as a step increase from about 100 to 250 N·m. We conducted 10 trials and computed the mean and standard deviation of the peak torque and peak power for each trial.

We also performed a test intended to evaluate the torque errors that would arise from unexpected disturbances to toe position. We expected that high series stiffness in this system might have provided high bandwidth at the cost of higher sensitivity to position disturbances, for example during initial toe contact with the ground. We placed the toes on opposite ends of a seesaw-like testing jig such that toe forces were equal and toe motions were equal and opposite (Video 2). We then applied a 0 to 25 Hz chirp in medial toe position, oscillating between 0° and 5° of plantarflexion (or 0 and 0.012 m of toe tip displacement) and commanded a constant desired torque of 30 N·m to the lateral toe. We transformed the amplitude of the resulting torque error into the frequency domain using a Fast Fourier Transform, reported as a percent of the constant desired torque magnitude. We calculated the frequency at

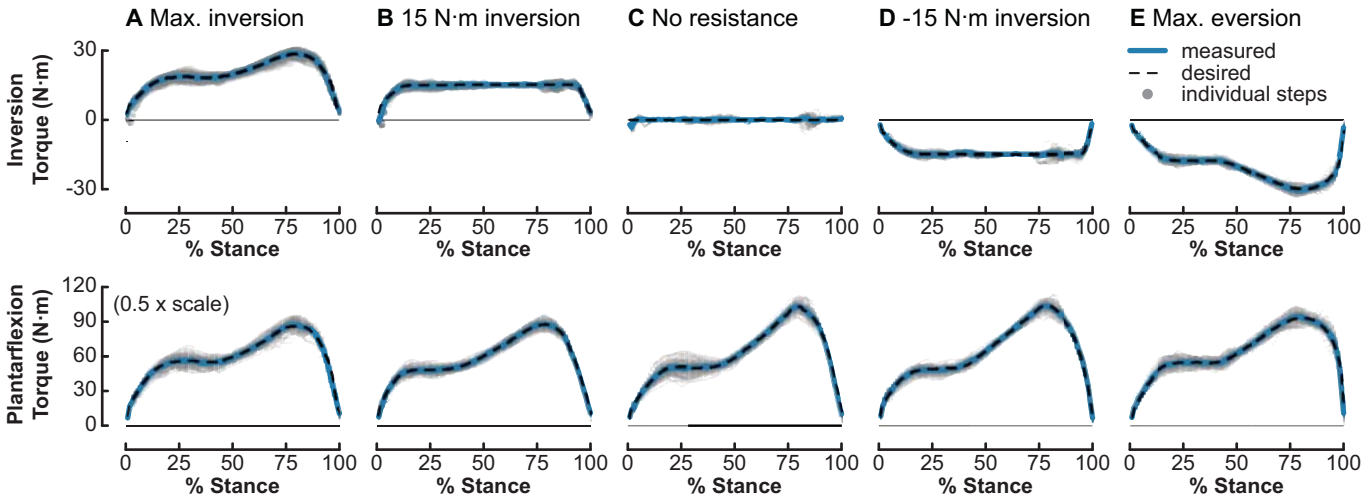

Fig. 8. Torque tracking during walking experiments. Desired ankle inversion torque was set to **A** Maximum, **B** 15 N·m, **C** zero, **D** -15 N·m, and **E** Maximum Negative, while desired plantarflexion torque was a consistent function of ankle plantarflexion angle. Maximum and Maximum Negative allowable inversion torque were limited by desired plantarflexion torque, since toe ground reaction forces could not become negative. In each 100-stride trial, measured torque closely matched desired torque, with RMS errors of at most 3.7 N·m in plantarflexion and 1.1 N·m in inversion-eversion across conditions. Differences between average torque and individual-step torques were dominated by changes in desired torque arising from natural variability in the subject's gait pattern.

which error rose above 30% of the desired torque, analogous to the -3 dB (70% amplitude) criteria used in bandwidth tests.

C.2 Walking Demonstration Methods:

We performed two sets of walking trials to evaluate torque tracking performance under realistic conditions. In the first set of trials, one subject (67 kg, 1.77 m tall, 23 yrs, male) without amputation wore the device using a simulator boot [47]. We used minimal Bowden cables, about 2 m in length, for best torque tracking performance. Five walking trials were conducted in which desired inversion-eversion torque was commanded as: Maximum, 15 N·m, 0 N·m, -15 N·m, and Maximum Negative. The magnitudes of Maximum and Maximum Negative inversion torque were proportional to plantarflexion torque at each instant in time. Using the simulator boot allowed these large torques to be applied comfortably.

In the second set of trials, one subject with unilateral transtibial amputation (89 kg, 1.72 m tall, 26 yrs, male) wore the device using their prescribed socket. We used extended Bowden cables, about 4 m in length, for improved range of movement on the treadmill and reduced interference between off-board emulator components and biomechanics data collection equipment. Three walking trials were conducted in which desired inversion-eversion torque was commanded as: 10 N·m, 0 N·m and -10 N·m. These magnitudes were chosen to maximize range of torque without causing discomfort in the residual limb from repeated applications of torque in one direction (Video 3).

In both sets of trials, subjects walked on a treadmill at 1.25 m·s^{-1} for 100 steady-state strides in each condition. We normalized each step to percent stance period and calculated an average step for each condition. We characterized torque tracking error as both the RMS error across the entire trial and as the RMS error of the average step. We did not measure human biomechanical response, since this study was intended to evaluate performance of the robotic system and not the effects of a proposed intervention.

III. Results

Benchtop tests with a fixed load determined measurement error, rise time and closed-loop torque bandwidth. The root mean squared (RMS) torque measurement errors for medial and lateral toes were 1.64 N·m and 2.43 N·m, respectively, following calibration (Fig. 5A&B). The 90% rise and fall times between 0 and 180 N·m in plantarflexion torque were 0.033 $\pm$ 0.001 s and 0.024 $\pm$ 0.001 s (mean $\pm$ s.d.), with 0.5% and 1.6% overshoot, respectively (Fig. 5C). The 90% rise and fall times between -20 to 20 N·m in inversion-eversion torque were 0.026 $\pm$ 0.002 s and 0.027 $\pm$ 0.002 s, with 3.0% and 3.2% overshoot, respectively (Fig. 5D). With desired plantarflexion torque oscillating between 10 and 90 N·m, the -3 dB magnitude and 45° phase margin crossover frequencies were 27.2 $\pm$ 0.2 Hz and 20.3 $\pm$ 0.3 Hz, respectively (Fig. 5E). With desired inversion-eversion torque oscillating between -20 and 20 N·m, the -3 dB magnitude and 45° phase margin crossover frequencies were 29.8 $\pm$ 0.2 Hz and 23.8 $\pm$ 0.3 Hz, respectively (Fig. 5F).

Benchtop tests with a compliant load characterized peak joint torque, velocity and power. Peak measured plantarflexion torque was 248 $\pm$ 6 N·m (Fig. 6A). Peak measured plantarflexion velocity was 26.3 $\pm$ 1.1 rad·s^{-1} (Fig. 6B). Peak mechanical power was 3,050 $\pm$ 240 W (Fig. 6C). During the period of peak power output the tether was being stretched, thereby absorbing energy and not contributing to peak power through return of stored energy.

When we applied a 0.012 m amplitude chirp disturbance in toe endpoint position and commanded a constant desired torque of 30 N·m, torque error was less than 30% up to a disturbance frequency of 18 Hz (Fig. 7). This disturbance frequency and amplitude are similar to unexpected contact with stiff ground at a rate of 1.4 m·s^{-1}.

In the first set of walking trials, the non-amputee subject walked comfortably with the prosthesis on a short tether while

TABLE I
TORQUE TRACKING ERRORS DURING 100 STEPS OF WALKING WITH VARIOUS VALUES OF DESIRED INVERSION-EVERSION TORQUE.

CASE 1: NON-AMPUTEE WITH SIMULATOR BOOT AND SHORT TETHER

	Plantarflexion Torque Tracking				*Inversion-Eversion Torque Tracking*			
Inversion-eversion torque	RMS error	$\%\tau_{max}$	AVG RMS error	$\%\tau_{max}$	RMS error	$\%\tau_{max}$	AVG RMS error	$\%\tau_{max}$
τ_{inv} = Maximum	3.2 ± 1.1 N·m	3.7%	1.3 N·m	1.6%	1.1 ± 0.4 N·m	3.8%	0.4 N·m	1.6%
τ_{inv} = -15 N·m	1.9 ± 0.4 N·m	2.2%	0.7 N·m	0.8%	0.9 ± 0.2 N·m	5.9%	0.7 N·m	4.4%
τ_{inv} = 0	2.9 ± 1.7 N·m	2.8%	0.6 N·m	0.6%	0.8 ± 0.2 N·m	-	0.5 N·m	-
τ_{inv} = -15 N·m	2.9 ± 0.8 N·m	2.8%	0.9 N·m	0.8%	0.8 ± 0.2 N·m	5.6%	0.3 N·m	2.1%
τ_{inv} = Negative Maximum	3.0 ± 0.9 N·m	3.3%	1.3 N·m	1.4%	1.0 ± 0.3 N·m	3.3%	0.4 N·m	1.6%

CASE 2: TRANSTIBIAL AMPUTEE WITH LONG TETHER

	Plantarflexion Torque Tracking				*Inversion-Eversion Torque Tracking*			
Inversion-eversion torque	RMS error	$\%\tau_{max}$	AVG RMS error	$\%\tau_{max}$	RMS error	$\%\tau_{max}$	AVG RMS error	$\%\tau_{max}$
τ_{inv} = -10 N·m	4.7 ± 1.0 N·m	3.9%	1.3 N·m	1.1%	1.5 ± 0.3 N·m	14.6%	0.7 N·m	6.4%
τ_{inv} = 0	5.1 ± 1.2 N·m	4.2%	1.5 N·m	1.3%	1.1 ± 0.3 N·m	-	0.2 N·m	-
τ_{inv} = -10 N·m	4.8 ± 1.0 N·m	3.9%	1.2 N·m	1.0%	1.3 ± 0.3 N·m	13.2%	0.3 N·m	2.5%

TABLE II
PERFORMANCE COMPARISON CHART

Parameter		Emulator	Best of Prior Devices	Human
Mass		0.7 kg	1.13 kg [21]	1.0 kg [49]
Range of Motion	pf.	-20° to 30°	-20° to 25° [50]	-20° to 50° [43]
	inv.	±30°	-6° to 22° [20]	±28° [43]
Speed		26 rad·s^{-1}	5 rad·s^{-1} [50]	15 rad/s* [51]
Torque	pf.	250 N·m	180 N·m [4]	400 N·m* [51]
	inv.	±30 N·m	±30 N·m [20]	±50 N·m [52]
Power		3,050 W	360 W [4]	1,200 W* [51]
Bandwidth	pf.	20 Hz	3.8 Hz [50]	6 Hz [53]
	inv.	24 Hz	1.8 Hz [20]	6 Hz [53]
Dist. Rejection		18 Hz	-	-
Maximum RMS Tracking Error	pf.	5.1 Nm	-	-
	inv.	1.5 Nm	-	-

pf. is plantarflexion, inv. is eversion. * is estimated. - is unavailable.

five levels of constant desired inversion-eversion torque were applied (Fig. 8). Peak inversion torques during Maximum and Maximum Negative conditions were about 30 N·m and -30 N·m, respectively. Torque tracking errors in both plantarflexion and inversion-eversion directions were low, with maximum RMS errors of 3.2 N·m (3.7% of peak) in plantarflexion torque and 1.1 N·m (3.8% of peak) in inversion-eversion torque, across all conditions (Table I).

In the second set of walking trials, the transtibial amputee subject walked comfortably with the prosthesis on the longer tether while three lower levels of constant desired inversion-eversion torque were applied. Torque tracking errors in both plantarflexion and inversion-eversion directions were higher in these trials, with maximum RMS errors of 5.1 N·m (4.2% of peak) in plantarflexion torque and 1.5 N·m (14.6% of peak) in inversion-eversion torque (Table I). Higher percent error in inversion-eversion torque in this set of trials was primarily the result of lower peak torque (±10 N·m vs. ±30 N·m).

IV. DISCUSSION

We designed, built and tested an ankle-foot prosthesis system with torque control in both plantarflexion and inversion-eversion directions. Relative to the performance of prior ankle-foot prostheses and the intact human limb (Table II), the end-effector is lightweight, yet provides high torque, speed and power. The system has both high closed-loop torque bandwidth and low torque errors in the presence of unexpected toe displacements. During walking trials with an amputee subject, a wide range of inversion-eversion torque values were tracked with low error. Taken as a whole, these results demonstrate the versatility of the ankle-foot prosthesis emulator and its suitability for haptic emulation of prostheses with both pitch and roll degrees of freedom.

This prosthesis emulator is versatile, with mass, size, torque, speed and power that compare favorably to normal ankle-foot function and to other active prostheses (Table II). The end-effector has about 60% of the mass of a typical human foot [49], similar to the mass of passive ankle-foot prostheses [17] and about a third of the mass of other human-subject tested tethered [4, 20, 54] and untethered [2, 55–57] powered ankle-foot prostheses. The end-effector has dimensions similar to a human foot [41]. Peak measured plantarflexion and inversion-eversion torques were 50% and 230% greater, respectively, than the peak values observed at the human ankle joint during walking and running among typical males [27, 58, 59]. Peak measured plantarflexion torques were about 40% greater than in other devices with powered plantarflexion [2, 4, 55–57], and peak inversion-eversion torques were equivalent to those in other devices with powered inversion-eversion [20]. Peak joint velocity and power were each about three times greater than peak values observed at the ankle joint during normal walking and running [58, 59], and an order of magnitude greater than in previous powered devices [4, 50, 55–57].

The responsiveness of this device also compares favorably to human musculature and to other active prostheses, allowing accurate rendering of virtual devices. The system has high closed-loop torque bandwidth, up to 24 Hz, a limiting factor in the fidelity of haptic emulation [60–62]. Measured bandwidth was about four times that of human ankle muscles [53].

This is nearly twice the bandwidth of our previous ankle-foot prosthesis system [29], five times that of untethered electric prostheses [63], and about ten times that of similar systems using pneumatic muscles [4, 64]. Inversion-eversion step response time was about five times faster than prior systems with on-board actuation [20]. Torque disturbances due to unexpected toe movements could be rejected at high frequencies, an indication of robustness during unpredictable human interactions [65]. Torque tracking errors were below 30% in the presence of disturbances at up to twice the peak voluntary oscillation frequencies of the human ankle [66]. This disturbance rejection cutoff frequency corresponded to more than 83% of the frequency content of the prosthetic ankle joint angle during walking trials.

Both plantarflexion and inversion-eversion torques were tracked with low error during walking across a range of conditions, demonstrating the effectiveness of this system for prosthesis emulation experiments. Absolute torque tracking errors were low across all conditions and outcomes, with values similar to those observed for humans attempting to maintain constant isometric ankle joint torque [67]. Maximum observed plantarflexion and inversion-eversion torque errors were 2% and 5% of system torque capacity, respectively. In most cases errors were also small relative to peak desired torques, although percent error naturally approached infinity as desired inversion-eversion torque approached zero.

The addition of an ankle inversion-eversion degree of freedom may allow for higher walking speed [18] or reduced reliance on foot placement for balance [20]. The improved performance afforded by our system has further allowed demonstrations of new techniques for reducing balance-related effort, such as through online modulation of inversion stiffness characteristics [68], owing to its precise control and programmability [39]. With these characteristics, this device can be used to test numerous control algorithms developed for wide range of k-level individuals with below knee amputation.

Both absolute and relative torque errors were greater in tests with the longer tether and the amputee subject. Absolute tracking errors were about 50% higher in both plantarflexion and inversion-eversion, likely due to increased compliance, friction, stiction, delays and other nonlinearities with the longer Bowden cable. This decrease in absolute performance could also relate to differences between amputee and non-amputee gait characteristics, but such differences were not apparent in any measured kinetics or kinematics data. Use of shorter, straighter Bowden cables is therefore warranted where possible, for example by mounting motors above the subject [69]. Other improvements to the Bowden cable transmission, for example using intermediate components with lower friction and fewer nonlinearities, could yield simultaneous improvements in torque tracking, range on the treadmill, and convenience. Additionally, the effect of compliance on control performance can be systematically examined and the information can be used to improve control.

The substantially higher percent inversion-eversion torque error observed in trials with the amputee subject are largely the result of lower desired torques. When maximum inversion-eversion torques were applied on each step, the subject reported discomfort in their residual limb. It is not clear whether the full range of inversion-eversion torque capacity of the present system is necessary for tests involving subjects with amputation. Intermittent application of higher torques may be allowable, and peak torques may vary across individuals.

Although this design does not include an explicit series spring in the end-effector, disturbance rejection was relatively high and torque tracking errors were low during walking. It appears that series elasticity provided by stretch in the Bowden cable transmission sufficiently decoupled the toes from the inertia of the motor. This has not been the case for all emulator end-effectors we have tested. In pilot tests with an ankle exoskeleton [33], we found that removing the coil spring at the ankle joint led to increased torque tracking errors. Differences may be related to the types of disturbance provided by the human in these cases; having muscles in parallel with the actuator, as with an exoskeleton, may produce larger or higher-frequency variations in interaction torques than when a prosthesis is placed in series with the limb.

Torque measurement was also not adversely affected by lack of a series spring in this system. Measuring torque using spring deflection [28, 70] can reduce electromagnetic noise compared to strain gauges [38]. In this case, the amplified strain gauge bridge voltage exhibited noise in the kHz range, but this was easily removed by sampling at high frequency and low-pass filtering. Utilizing Bowden cable compliance therefore reduced the mass and complexity of the end-effector without negatively affecting torque tracking or measurement.

Instrumenting the toes with strain gauges also resulted in lower complexity and more accurate torque measurement than the use of load cells in this case. In an earlier revision of this design, Bowden cable tension was sensed using pushbutton load cells with a through hole at the conduit termination (inside the cyan elements in Fig. 1B). This resulted greater mass, undesired loads from the cable, and hysteresis due to friction and shifting at the termination.

Using two toes for inversion-eversion results in a simple, lightweight structure, but does not allow simple measurement of frontal-plane motions or torques. The angle of the shank with respect to vertical in the frontal plane cannot be calculated from the angles of the medial and lateral toes alone (unless they are equal), since rotation about the line between toe contact points is not captured by joint angles. More sensory information, such as the pitch angle of the prosthesis frame, is required. A similar problem arises if inversion-eversion torque is defined about an axis in the direction of travel. In a laboratory setting, this issue can be overcome by measuring shank angle directly with motion capture equipment. Solutions that would be suitable for autonomous devices include measuring shank angle with an inertial measurement unit or (actively) maintaining heel contact throughout stance to obtain the missing configuration-related measurement.

The prosthesis emulator has high-fidelity control over the mediolateral location of the center of pressure during stance, but would require an additional active degree of freedom to usefully control fore-aft center of pressure location. Humans seem to regulate the path of the center of pressure during walking [71], making this a potentially interesting signal

for manipulation. In this system, the mediolateral center of pressure can be controlled through inversion-eversion torque when both toes are in contact with the ground. In the fore-aft direction, the center of pressure can only be controlled when the heel is also in contact. Since the heel is passive, contact is maintained only for a limited range of shank and toe configurations and heel force cannot be controlled. Active torque control of the heel would resolve these issues, as could the inclusion of additional human-like structural features.

Although we only present data for tests with two subjects, we expect similar haptic emulation performance for a wide range of individuals and protocols. Human response to robotic intervention can depend strongly upon subject characteristics [72, 73], but device behavior typically does not [74, 75]. Benchtop measurements are, of course, subject-independent. This study concerned the mechatronic performance of the prosthesis emulator, whereas future studies probing biomechanical response to different interventions will require multiple subjects with amputation. Future studies will also provide additional validation of the accuracy with which various prosthesis features, such as inversion-eversion compliance, can be rendered under various walking conditions, such as at slower and faster speeds.

This system provides excellent versatility within a laboratory environment, but cannot be used for community ambulation. This is a fundamental limitation of the approach compared to mobile devices. One implication is that acclimation to use of the device must take place in the laboratory, which places a practical limit on training time. Positive outcomes with some active prostheses have been achieved following several weeks of acclimation [2], although adequate adaptation times are not yet known. Use of a subject's prescribed prosthesis between training sessions could also cause interference effects, like those observed during manipulation of novel objects [76]. Some aspects of the dynamics of treadmill walking differ from those of overground walking [77], which could limit the applicability of some findings to community ambulation. For experimental protocols exploring the design and control of novel prostheses in a laboratory setting, however, this system provides better performance than mobile devices.

V. Conclusions

We have described the design of a tethered ankle-foot prosthesis emulator system with independent control over plantarflexion and inversion-eversion torque.

Device performance: The results of benchtop tests and experiments during human walking provide a detailed characterization of system dynamics and performance. The mass, range of motion, peak speed, peak torque, peak power, closed-loop torque bandwidth and disturbance rejection of this system all demonstrate substantial improvements compared to prior devices. Walking trials with a participant with unilateral transtibial amputation demonstrated the practicality of the system and the capacity to produce a large range of inversion-eversion torques with low error during amputee gait.

These properties make the system suitable for haptic emulation of a wide variety of prostheses with pitch and roll degrees of freedom.

Application: We expect this system to enable future experiments that provide insights into the role of inversion-eversion torque control on walking balance for individuals with amputation. The effects of passive inversion-eversion stiffness could be isolated, providing insights into the trade-offs between sensitivity to uneven terrain and balance recovery on flat surfaces. New types of quasi-active prosthesis behavior could be explored, including designs that cancel out ground irregularities by matching the shape of the walking surface. Mediolateral center of pressure trajectories that match those observed in non-amputee gait could be applied and their effects on balance tested. More sophisticated feedback control approaches could be developed, including once-per-step modulation of inversion-eversion torque in a manner similar to the approach to controlling push-off work that has proven effective in reducing balance-related effort [34].

Potential impact: These and other prosthesis features that utilize inversion-eversion torque have the potential to enhance amputee balance, and the prosthesis emulator described here is uniquely well-suited to their investigation. Successful approaches could later be transferred into specialized, mobile commercial devices, with reduced development risk [30]. Other applications include rendering virtual devices to users as part of the clinical prescription process [31, 37], and basic science experiments probing the nature of human locomotion [47].

VI. Acknowledgments

The authors thank Josh Caputo, Tyler del Sesto and Faith Quist for their contributions to system development and data collection, and Zach Batts, Winton Zheng and Tanuf Tembulkar for contributions to system development.

References

[1] F. Sup *et al.*, "Self-contained powered knee and ankle prosthesis: Initial evaluation on a transfemoral amputee," in *Proc. Int. Conf. Rehab. Rob.*, pp. 638–644, 2009.

[2] H. M. Herr and A. M. Grabowski, "Bionic ankle-foot prosthesis normalizes walking gait for persons with leg amputation," *Proc. Roy. Soc. Lon. B*, vol. 279, pp. 457–464, 2012.

[3] E. R. Esposito, J. M. A. Whitehead, and J. M. Wiken, "Step-to-step transition work during level and inclined walking using passive and powered anklefoot prostheses," *Prosth. Orth. Int.*, p. 0309364614564021, 2015.

[4] S. Huang, J. P. Wensman, and D. P. Ferris, "An experimental powered lower limb prosthesis using proportional myoelectric control," *J. Med. Dev.*, vol. 8, p. 024501, 2014.

[5] A. M. Dollar and H. Herr, "Lower extremity exoskeletons and active orthoses: challenges and state-of-the-art," *Trans. Rob.*, vol. 24, pp. 144–158, 2008.

[6] M. Goldfarb, B. E. Lawson, and A. H. Schultz, "Realizing the promise of robotic leg prostheses," *Sci. Trans. Med.*, vol. 5, pp. 1–6, 2013.

[7] P. Cherelle *et al.*, "Advances in propulsive bionic feet and their actuation principles," *Adv. Mech. Eng.*, vol. 6, p. 984046, 2014.

[8] A. D. Kuo, "Stabilization of lateral motion in passive dynamic walking," *Int. J. Rob. Res.*, vol. 18, pp. 917–930, 1999.

[9] S. M. Bruijn *et al.*, "The effects of arm swing on human gait stability," *J. Exp. Biol.*, vol. 213, pp. 3945–3952, 2010.

[10] Y. Wang and M. Srinivasan, "Stepping in the direction of the fall: the next foot placement can be predicted from current upper body state in steady-state walking," *Biol. Let.*, vol. 10, p. 20140405, 2014.

[11] T. IJmker *et al.*, "Can external lateral stabilization reduce the energy cost of walking in persons with a lower limb amputation?" vol. 40, pp. 616–621, 2014.

[12] N. Matsusaka, "Control of the medial-lateral balance in walking," *Acta Orthop. Scand.*, vol. 57, pp. 555–559, 1986.

[13] D. A. Winter, "Human balance and posture control during standing and walking," *Gait Post.*, vol. 3, pp. 193–214, 1995.

[14] M. Vlutters, E. H. F. V. Asseldonk, and H. V. der Kooij, "Center of mass velocity-based predictions in balance recovery following pelvis perturbations during human walking," *J. Exp. Biol.*, vol. 219, pp. 1514–1523, 2016.

[15] A. L. Hof *et al.*, "Control of lateral balance in walking: Experimental findings in normal subjects and above-knee amputees," *Gait Post.*, vol. 25, pp. 250–258, 2007.

[16] College Park, "College Park - Trustep," September, 2014. URL: http://www.college-park.com/prosthetics/trustep.

[17] Össur, "Vari-Flex," September, 2014. URL: http://www.ossur.com/prosthetic-solutions/products/feet/ feet/ vari-flex.

[18] a. J. M. A. Gates, Deanna H. and J. M. Wilken, "Kinematic comparison of walking on uneven ground using powered and unpowered prostheses." *Clinical Biomechanics*, vol. 28, pp. 467–472, 2013.

[19] W. C. Miller, M. Speechley, and B. Deathe, "The prevalence and risk factors of falling and fear of falling among lower extremity amputees," *Arch. Phys. Med. Rehab.*, vol. 82, pp. 1031–1037, 2001.

[20] J. T. Panzenbeck and G. K. Klute, "A powered inverting and everting prosthetic foot for balance assistance in lower limb amputees," vol. 24, pp. 175–180, 2012.

[21] E. M. Ficanha *et al.*, "Design and preliminary evaluation of a two dofs cable-driven anklefoot prosthesis with active dorsiflexionplantarflexion and inversioneversion." *Frontiers in bioengineering and biotechnology*, p. 4, 2016.

[22] R. D. Bellman, M. A. Holgate, and T. G. Sugar, "SPARKy 3: Design of an active robotic ankle prosthesis with two actuated degrees of freedom using regenerative kinetics," in *Proc. BioRob*, pp. 511–516, 2008.

[23] M. Wisse and A. L. Schwab, "Skateboards, bicycles, and three-dimensional biped walking machines: velocity-dependent stability by means of lean-to-yaw coupling." *Int. J. Rob. Res.*, vol. 24, pp. 417–429, 2005.

[24] M. Venkadesan *et al.*, "Stiffness of the human foot and evolution of the transverse arch." *arXiv preprint*, 2017, arXiv:1705.10371.

[25] A. Roy *et al.*, "Robot-aided neurorehabilitation: a novel robot for ankle rehabilitation," *Trans. Rob.*, vol. 25, pp. 569–582, 2009.

[26] J. J. Eng and D. A. Winter, "Kinetic analysis of the lower limbs during walking: what information can be gained from a three-dimensional model?" *J. Biomech.*, vol. 28, pp. 753–758, 1995.

[27] A. E. Hunt, R. M. Smith, and M. Torode, "Extrinsic muscle activity, foot motion and ankle joint moments during the stance phase of walking," *Foot Ankle*, vol. 22, pp. 31–41, 2001.

[28] J. M. Caputo and S. H. Collins, "An experimental robotic testbed for accelerated development of ankle prostheses," in *Proc. Int. Conf. Rob. Autom.*, pp. 2630–2635, 2013.

[29] J. M. Caputo and S. H. C. Collins, "A universal ankle-foot prosthesis emulator for experiments during human locomotion," *J. Biomech. Eng.*, vol. 136, p. 035002, 2014.

[30] S. H. Collins, "What do walking humans want from mechatronics?" in *Proc. ICM*, pp. 24–27, 2013.

[31] S. H. Collins, J. M. Caputo, and P. G. Adamczyk, "Emulating prosthetic feet during the prescription process to improve outcomes and justifications," in *Proc. ARSO*, pp. 1–2, 2014.

[32] K. A. Witte, J. Zhang, and R. W. Jackson, "Design of two lightweight torque-controlled ankle exoskeletons," in *Proc. Int. Conf. Rob. Autom.*, pp. 1223–1228, 2015.

[33] J. Zhang, C. C. Cheah, and S. H. Collins, "Experimental comparison of torque control methods on an ankle exoskeleton during human walking," in *Proc. Int. Conf. Rob. Autom.*, pp. 5584–5589, 2015.

[34] M. Kim and S. H. Collins, "Once-per-step control of ankle-foot prosthesis push-off work reduces effort associated with balance during human walking," *J. NeuroEng. Rehabil.*, vol. 12, p. 43, 2015.

[35] R. W. Jackson and S. H. Collins, "An experimental comparison of the relative benefits of work and torque assistance in ankle exoskeletons," *J. Appl. Physiol.*, vol. in press, 2015.

[36] S. H. Collins, M. B. Wiggin, and G. S. Sawicki, "An exoskeleton that uses no energy yet reduces the metabolic cost of human walking," *Nature*, vol. 522, pp. 212–215, 2015.

[37] J. M. Caputo, P. G. Adamczyk, and S. H. Collins, "Informing ankle-foot prosthesis prescription through haptic emulation of candidate devices," in *Proc. Int. Conf. Rob. Autom.*, pp. 6445–6450, 2015.

[38] G. Pratt and M. Williamson, "Series elastic actuators," in *Proc. Int. Conf. Intel. Rob. Sys.*, 1995.

[39] M. Kim, "Ankle controller design for robotic ankle-foot prostheses to reduce balance-related effort during walking using a dynamic walking approach," PhD dissertation, Carnegie Mellon University, Department of Mechanical Engineering, 2015, Advisor: Steve H. Collins.

[40] S. H. Collins *et al.*, "An ankle-foot prosthesis emulator with control of plantarflexion and inversion-eversion torque," in *Proc. Int. Conf. Rob. Autom.*, pp. 1210–1216, 2015.

[41] M. R. Hawes and D. Sovak, "Quantitative morphology of the human foot in a North American population," *Ergonomics*, vol. 37, pp. 1213–1226, 1994.

[42] D. A. Winter, *The Biomechanics and Motor Control of Human Gait: Normal, Elderly and Pathological*. Waterloo, Canada: Waterloo Biomechanics, 1991.

[43] A. Roaas and G. B. J. Andersson, "Normal range of motion of the hip, knee and ankle joints in male subjects, 30–40 years of age," vol. 53, pp. 205–208, 1982.

[44] H. Vallery *et al.*, "Compliant actuation of rehabilitation robots," *Rob. Autom. Mag.*, vol. 15, pp. 60–69, 2008.

[45] M. Kim *et al.*, "CAD models and bill of materials," September, 2016. URL: biomechatronics.cit.cmu.edu/publications/Kim_2016_TRO---CAD_Files.zip.

[46] S. H. Collins, "Carnegie Mellon University Experimental Biomechatronics Laboratory – Publications," September, 2016. URL: biomechatronics.cit.cmu.edu/publications.html.

[47] J. M. Caputo and S. H. Collins, "Prosthetic ankle push-off work reduces metabolic rate but not collision work in non-amputee walking," *Nat. Sci. Rep.*, vol. 4, p. 7213, 2014.

[48] K. Warwick, *An Introduction to Control Systems*, 2nd ed. Singapore: World Scientific, 1996.

[49] D. A. Winter, *Biomechanics and Motor Control of Human Movement*, 2nd ed. Toronto, Canada: John Wiley & Sons, Inc., 1990.

[50] S. K. Au and H. Herr, "Powered ankle-foot prosthesis improves walking metabolic economy," *Trans. Rob.*, vol. 25, pp. 51–66, 2009.

[51] B. M. Ashby and S. L. Delp, "Optimal control simulations reveal mechanisms by which arm movement improves standing long jump performance," vol. 39, pp. 1726–1734, 2006.

[52] R. A. O. C. H. Ashton-Miller, James A. and E. M. Wojtys, "What best protects the inverted weightbearing ankle against further inversion? evertor muscle strength compares favorably with shoe height, athletic tape, and three orthoses," *Am. J. Sports Med.*, vol. 24, pp. 800–809, 1996.

[53] P. Bawa and R. B. Stein, "Frequency response of human soleus muscle," *J. Neurophys.*, vol. 39, pp. 788–793, 1976.

[54] E. M. Ficanha *et al.*, "Ankle angles during step turn and straight walk: Implications for the design of a steerable ankle-foot prosthetic robot," in *Proc. DSCC*, pp. 1–5, 2013.

[55] J. K. Hitt *et al.*, "An active foot-ankle prosthesis with biomechanical energy regeneration," *J. Med. Dev.*, vol. 4, 2010.

[56] A. H. Shultz *et al.*, "Preliminary evaluation of a walking controller for a powered ankle prosthesis," in *Proc. Int. Conf. Rob. Autom.*, pp. 4823–4828, 2013.

[57] P. Cherelle *et al.*, "Design and validation of the ankle mimicking prosthetic (AMP-) foot 2.0," *Trans. Neural Syst. Rehabil. Eng.*, vol. 22, pp. 138–148, 2014.

[58] M. Whittle, *Gait Analysis: An Introduction*. Oxford, United Kingdom: Butterworth-Heinemann, 1996.

[59] T. F. Novacheck, "The biomechanics of running," *Gait Post.*, vol. 7, pp. 77–95, 1998.

[60] C. Abul-Haj and N. Hogan, "An emulator system for developing improved elbow-prosthesis designs," *Trans. Biomed. Eng.*, vol. 9, pp. 724–737, 1987.

[61] B. Hannaford and A. Okamura, "Haptics," in *Springer Handbook of Robotics*, pp. 719–739. Heidelberg, Germany: Springer Berlin, 2008.

[62] P. G. Griffiths, R. B. Gillespie, and J. S. Freudenberg, "A fundamental linear systems conflict between performance and passivity in haptic rendering," *Trans. Rob.*, vol. 27, pp. 75–88, 2011.

[63] S. K. Au, J. Weber, and H. Herr, "Biomechanical design of a powered ankle-foot prosthesis," in *Proc. Int. Conf. Rehab. Rob.*, pp. 298–303, 2007.

[64] K. E. Gordon, G. S. Sawicki, and D. P. Ferris, "Mechanical performance of artificial pneumatic muscles to power an ankle-foot orthosis," *J. Biomech.*, vol. 39, pp. 1832–1841, 2006.

[65] N. Hogan, "Impedance control: An approach to manipulation," in *Amer. Contr. Conf.*, pp. 304–313, 1984.

[66] G. C. Agarwal and G. L. Gottlieb, "Oscillation of the human ankle joint in response to applied sinusoidal torque on the foot," *J Physiol.*, vol. 268, pp. 151–176, 1977.

[67] N. Vuillerme and M. Boisgontier, "Muscle fatigue degrades force sense

at the ankle joint," *Gait Post.*, vol. 28, pp. 521–524, 2008.
[68] T. Chen *et al.*, "Inversion-eversion stiffness of ankle-foot prosthesis affects amputee's balance-related effort during walking." in *Proc. Dynamic Walking*, 2015.
[69] J. B. Andersen and T. Sinkjær, "An actuator system for investigating electrophysiological and biomechanical features around the human ankle joint during gait," *Trans. Rehab. Eng.*, vol. 3, pp. 299–306, 1995.
[70] J. Pratt, B. Krupp, and C. Morse, "Series elastic actuators for high fidelity force control," *Indust. Rob: Int. J.*, vol. 29, pp. 234–241, 2002.
[71] A. H. Hansen, D. S. Childress, and E. H. Knox, "Roll-over shapes of human locomotor systems: effects of walking speed," vol. 19, pp. 407–414, 2004.
[72] K. E. Zelik *et al.*, "Systematic variation of prosthetic foot parameter affects center-of-mass mechanics and metabolic cost during walking," *Trans. Neural Syst. Rehabil. Eng.*, vol. 19, pp. 411–419, 2011.
[73] A. D. Segal *et al.*, "The effects of a controlled energy storage and return prototype prosthetic foot on transtibial amputee ambulation," *Hum. Mov. Sci.*, vol. 31, pp. 918–931, 2012.
[74] M. J. Major *et al.*, "Amputee independent prosthesis properties–A new model for description and measurement," *J. Biomech.*, vol. 44, pp. 2572–2575, 2011.
[75] P. G. Adamczyk, M. Roland, and M. E. Hahn, "Novel method to evaluate angular stiffness of prosthetic feet from linear compression tests," *J. Biomech. Eng.*, vol. 135, p. 104502, 2013.
[76] Q. Fu and M. Santello, "Retention and interference of learned dexterous manipulation: interaction between multiple sensorimotor processes," *J. Neurophys.*, vol. 113, pp. 144–155, 2015.
[77] J. B. Dingwell *et al.*, "Local dynamic stability versus kinematic variability of continuous overground and treadmill walking," *J. Biomech. Eng.*, vol. 123, pp. 27–32, 2001.

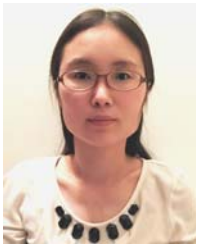

Myunghee Kim received her B.S. from Hayang University, Seoul, South Koreain 2002; M.S. degrees from Korea Advanced Institute of Science and Technology, Daejeon, South Korea, in 2004 and from Massachusetts Institute of Technology, Cambridge, USA, in 2006; and the Ph.D. degree from Carnegie Mellon University, Pittsburgh, PA, USA, in 2015, all in mechanical engineering. She was a control engineer in humanoid robotics at Samsung. She is a Postdoctoral Fellow with Wyss Institute for Biologically Inspired Engineering, and in the School of Engineering and Applied Sciences, Harvard University,Cambridge, MA, USA. Her research focus is on designing controllers for robotic devices to improve quality of life. She received Best Paper Award in the Medical Devices category at ICRA 2015.

Tianjian Chen is a PhD student in the Department of Mechanical Engineering at Columbia University, working in the Robotic Manipulation and Mobility Laboratory. He received his B.E. from Huazhong University of Science and Technology in 2013 and his M.S. from Carnegie Mellon University in 2015. His main research interest is robotics, especially in the context of rehabilitation.

Tianyao Chen is working toward his Ph.D degree in Biomedical Engineering at the Catholic University of America, where he is a research assistant at the National Rehabilitation Hospital. He received a B.S. in Aerospace Engineering from Beihang University in 2011 and an M.S. in Mechanical Engineering from Carnegie Mellon University in 2013. He worked as a research associate in Disney Research Pittsburgh. He currently studies upper-limb function restoration with robotic devices.

Steven H. Collins is an Associate Professor of Mechanical Engineering at Carnegie Mellon University, where he directs the Experimental Biomechatronics Laboratory and teaches courses on Design. He received his B.S. from Cornell University in 2002 and his Ph.D. from the University of Michigan in 2008. He performed postdoctoral research at T.U. Delft. He has published in *Science* and *Nature*. He is on the scientific board of Dynamic Walking, a recipient of the ASB Young Scientist Award, and was recently voted Mechanical Engineering Professor of the Year.